Tellus (1995), 47A, 548–560
Printed in Belgium – all rights reserved

TELLUS
ISSN 0280–6495

Hadley circulations and their rôles in the global angular momentum budget in two- and three-dimensional models

By MASAKI SATOH*, *Department of Mechanical Engineering, Saitama Institute of Technology, 1690 Fusaiji, Okabe, Saitama 369-02, Japan*, MASAYUKI SHIOBARA and MASAAKI TAKAHASHI, *Center for Climate System Research, University of Tokyo, Tokyo 153, Japan*

(Manuscript received 31 August 1994; in final form 18 April 1995)

ABSTRACT

Differences between the general circulations calculated in an axisymmetric 2-dimensional model (2D) and a non-axisymmetric 3-dimensional model (3D) are examined, particularly in terms of meridional circulations, angular momentum budget and zonal wind distributions. Circulations of the two models have similar properties in the low-latitudes. The Hadley cell exists in both cases, and their widths and intensities are comparable, though the cell is slightly stronger in the 3D model than in the 2D model especially in the terrestrial standard case. The surface winds in the Hadley regions are easterly, so that angular momentum is pumped from the surface to the atmosphere and transported to the upper layers and to the mid-latitudes. The most distinct difference is in cell shapes: the cell widths are broader at higher altitudes in 2D, while they do not depend on height in 3D. Circulations in the mid-latitudes are essentially different. In 2D, a symmetric multiple cellar structure exists. The cells are systematically moving equatorward, and they transport the angular momentum downward. The time averaged surface zonal winds almost vanish and a strong westerly shear appears in the mid-latitudes. In 3D, on the other hand, zonal mean winds in the mid-latitudes are westerly from the surface to the upper troposphere and the westerly shear is relatively weaker because of the existence of non-axisymmetric modes. This suggests that baroclinic waves in 3D efficiently transport angular momentum downward in comparison to the symmetric cells in 2D. Dependencies on the rotation rates show that the width of the Hadley cell becomes smaller as the rotation rate becomes faster. In the case of a faster rotation rate than the terrestrial rotation rate, the steady easterlies and westerlies alternately exist in the zonal mean surface winds of the mid- and high-latitudes, while a multiple jet structure exists at the tropopause level.

1. Introduction

Observationally, it is well-known that the Hadley cell in the low-latitudes and the Ferrel cell as a zonal average of baroclinic waves in the mid-latitudes play important rôles in the angular momentum budget of the general circulation (e.g., Palmén and Newton, 1969). Theoretical understandings of the Hadley circulations are promoted by using axisymmetric models (Schneider, 1977; Held and Hou, 1980). It is not sufficiently known, however, to what extent these symmetric circulations describe more realistic non-axisymmetric circulations; are the symmetric circulations regarded as basic states, in which baroclinic waves are regarded as just only perturbations; or are they completely different from the zonal mean states of asymmetric circulations? The straightest way to answer these questions is to compare the symmetric with the asymmetric circulations calculated with a numerical model under the same conditions.

* Corresponding author address: Dr. Masaki Satoh, Department of Mechanical Engineering, Saitama Institute of Technology, 1690 Fusaiji, Okabe, Saitama 369-02, Japan.

Williams (1988a, b) has compared the two kinds of circulations by using a general circulation model (GCM). In his results, the Hadley cells of symmetric experiments have more complex structures than those of asymmetric experiments (Williams, 1988a, Fig. 3; Williams, 1988b, Fig. 2). However, it is difficult to extract general conclusions from his results, since he used the "swamp" condition, i.e., a balance of energy is required at each surface boundary. Satoh (1994) has examined the symmetric circulations in a moist radiative-convective system by using a two-dimensional grid model, and found that the circulations become complicated under the swamp condition because of the strong interaction between the surface temperature and the atmospheric circulations; the upward branch of the cell separates into the "double ITCZ" structure. One may make a clearer comparison of the circulations if distributions of the surface temperature are externally fixed, rather than if they are variable. It is the aim of this study to calculate the symmetric and the asymmetric circulations with GCM under the prescribed surface temperature distribution, so as to investigate the particular roles of the Hadley and Ferrel cells in the angular momentum budget.

The general circulation model and initial and boundary conditions used in this study are briefly described in Section 2. Section 3 gives the numerical results. In particular, through dependencies on rotation rates, the position of the terrestrial circulation in the parametric space is examined, in order to explore to what extent the view of the terrestrial angular momentum budget applies to more general conditions. One can confirm many similarities between the axisymmetric results of this section and the results calculated by Satoh (1994) with a different kind of numerical model. Because of the use of the fixed surface temperature condition, axisymmetric and asymmetric results are not so different as those obtained by Williams, and it enables one to discuss the differences of the intensities and the widths of the Hadley cells between axisymmetric and asymmetric calculations. In Section 4, the relations of the Hadley and Ferrel cells and dependencies on the surface temperature distribution are discussed. In Section 5, the results obtained in this study are summarized with possible classifications of the Hadley cells and of the baroclinic zones, and related unresolved problems are commented upon.

2. Model

The GCM developed at the University of Tokyo (Numaguti, 1993)* is used to calculate the axisymmetric and non-axisymmetric states (here after, 2D and 3D, respectively). The resolution of 3D is T42 and 16 layers. In 2D, the modes of wave number zero alone are used in the longitudinal direction. The primitive equations with a σ-coordinate is used, with the levels given by $\sigma = 0.995$, 0.980, 0.950, 0.900, 0.830, 0.745, 0.650, 0.549, 0.454, 0.369, 0.295, 0.230, 0.175, 0.124, 0.074, and 0.021. The moist adjustment scheme, a simple non-grey radiation model, and the level II of Yamada and Meller boundary layer schemes are used as physical processes. The surface temperature is prescribed as

$$T_s = T_e - \Delta T \sin^2 \varphi, \tag{1}$$

in which $T_e = 300$ K, $\Delta T = 40$ K are used and φ is latitude. The surface is assumed to be wet, i.e., "an aqua planet model." The initial condition is a state at rest with a uniform temperature 250 K, except for 0.1 K perturbation of 3D at one grid point of the lowest level close to the equator. Both models are integrated under the same axisymmetric boundary condition. An equilibrium state of 3D is defined by a mean of 80–160 days, whereas an equilibrium state of 2D by a mean of 200–400 days.

3. Results

In this section, the differences of the general circulations in 2D and 3D are examined through their dependencies on the rotation rate Ω. Experiments for $\Omega/\Omega_0 = 0$, 1/4, 1/3, 1/2, 1, 2, 3, and 4 are carried out in both cases, and additional experiments for $\Omega/\Omega_0 = 1/8$ and 8 are performed only in 2D (Ω_0 is the terrestrial rotation rate). Among them, the results for $\Omega/\Omega_0 = 0$, 1/3, 1, and 3 are shown in this section*. Meridional mass stream functions and longitudinal mean zonal

* The model is a preliminary version of the Center for Climate System Research/National Institute for Environmental Studies (CCSR/NIES) general circulation model.

* As for the experiment $\Omega/\Omega_0 = 3$, a longer integration is required to obtain an equilibrium state. The equilibrium state is defined by a mean of 240–320 days.

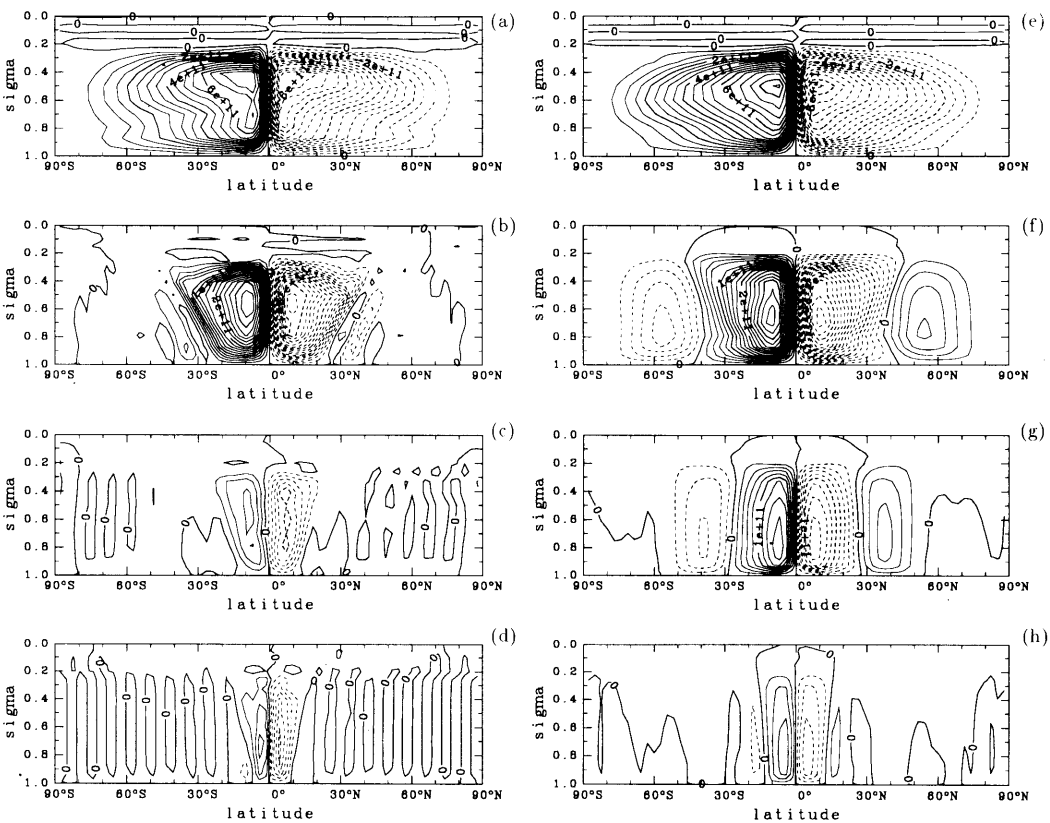

Fig. 1. Meridional distributions of mass stream functions for (a) 2D, $\Omega/\Omega_0 = 0$, (b) 2D, $\Omega/\Omega_0 = 1/3$, (c) 2D, $\Omega/\Omega_0 = 1$, (d) 2D, $\Omega/\Omega_0 = 3$, (e) 3D, $\Omega/\Omega_0 = 0$, (f) 3D, $\Omega/\Omega_0 = 1/3$, (g) 3D, $\Omega/\Omega_0 = 1$, and (h) 3D, $\Omega/\Omega_0 = 3$. Contour intervals are 5×10^{10} kg s^{-1} for (a) and (e), 2×10^{10} kg s^{-1} for (b)–(d), (f)–(h).

winds are shown in Figs. 1 and 2, respectively. Time variations of the zonal winds at the lowest level for $\Omega/\Omega_0 = 1$ are also shown in Fig. 3.

Results for 2D are very similar to those obtained with the two-dimensional grid model by Satoh (1994). Main characteristics, which are commonly produced in the different models and are thought to be physically significant, are described as follows. Clear direct cells (the Hadley cell) exist in each case (Figs. 1a–d). The cell is global for $\Omega = 0$, and is smaller as Ω becomes larger. The cells have trapezoidal shapes and the cell widths are broader at higher altitudes. In the mid-latitudes, there exists a multiple cellar structure (symmetric cells) moving equatorward. As for the meridional distributions of the zonal winds, they are easterly at the equator from the surface to the upper troposphere, while in the mid- and high-latitudes they are westerly except for the lowest levels (Figs. 2a–c). The width of the equatorial easterlies becomes smaller as Ω becomes larger, and it corresponds to the Hadley width at the lowest levels. In the the mid- and high-latitudes, pairs of the surface easterlies and westerlies, which are associated with the symmetric cells, are moving equatorward (Fig. 3a).

Different from Satoh (1994), weak indirect cells (the Ferrel cell) have appeared in Figs. 1c, d as a time average of the moving symmetric cells in the mid-latitudes. In addition, the meridional structure of the symmetric cells still remains even after time averaging as shown by Fig. 1b. The structure is similar to that of mesoscale convective systems or symmetric instability (Emanuel, 1979, 1982); phase lines are tilting poleward in the upper layers. In contrast to this, the phase tilt is very small in

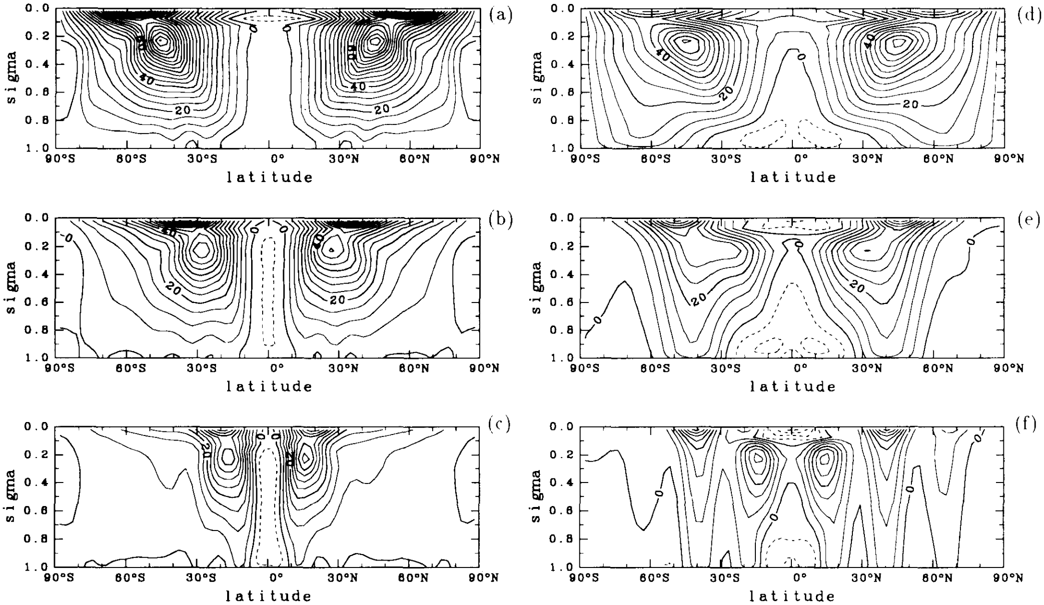

Fig. 2. Meridional distributions of zonal winds for (a) 2D, $\Omega/\Omega_0 = 1/3$, (b) 2D, $\Omega/\Omega_0 = 1$, (c) 2D, $\Omega/\Omega_0 = 3$, (d) 3D, $\Omega/\Omega_0 = 1/3$, (e) 3D, $\Omega/\Omega_0 = 1$, and (f) 3D, $\Omega/\Omega_0 = 3$. Contour intervals are 5 m s^{-1}.

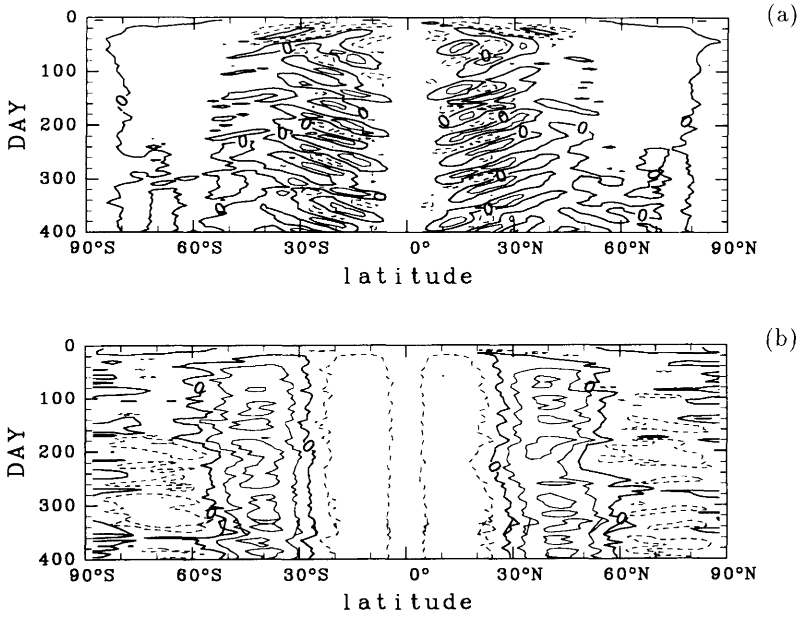

Fig. 3. Time variations of longitudinally averaged zonal winds at the surface for (a) 2D and (b) 3D for $\Omega/\Omega_0 = 1$. Contour intervals are 5 m s^{-1}.

Satoh. One of the reasons for the difference of the symmetric cells may be attributted to the different choice of diffusive processes between Satoh and the present study; the same parameterization as in 3D is used in the present 2D experiments, whereas the coefficients of viscosity are set to be a relatively small constant in Satoh. The moving symmetric cells do not exist in 3D; the Richardson number of the average states of the mid-latitudes is approximately 200, so that they are in a baroclinic unstable regime (Stone, 1966).

It should be noted that the usual framework of the symmetric instability (Stone, 1966; Emanuel, 1979) cannot be applied to the symmetric cells of 2D. In the present system, unstable stratification is always generated, since the surface temperature is externally fixed and the free atmosphere (troposphere) is cooled by radiation. There is possibility of occurrence of vertical convection in every latitudes. Because of the existence of moist process, convective motions organize on a large scale so that they are explicitly resolved in the model. The symmetric cells should be viewed as this kind of large-scale vertical convections.

As for the angular momentum budget, the inflow from the earth to the atmosphere (i.e., acceleration of the atmosphere) occurs in the region of the Hadley cell, in which the surface winds are easterly. The Hadley cell transports the angular momentum upward, and also transports it to the mid-latitude in the case of 2D: the poleward flows in the upper layers with larger angular momentums and the equatorward flows in the lower layers with relatively smaller angular momentums. In the mid-latitudes, the angular momentum is transferred principally by vertical diffusion from the Hadley cell to the symmetric cells, which in turn transport it downward. In order to maintain this cycle, the Hadley cell spreads over the upper layers of the symmetric cells. Thus, the width of the Hadley cell becomes broader in the higher altitudes. This is the essentially same view as that depicted by Eliassen (1951), though the Hadley and Ferrel cells are assumed to be steady in his consideration.

In 3D, dependencies of the Hadley cell on Ω have many similarities to 2D (Figs. 1e–h). Particularly, in the cases $\Omega/\Omega_0 = 0$, the stream functions almost agree with each other (Figs. 1a 2D and e 3D). For $\Omega/\Omega_0 = 1/3$, 1, and 3, indirect cells (the Ferrel cell) exist adjacent to the Hadley cells. As the rotation rate becomes faster, additional weak cells emerge on the polar sides of the Ferrel cells: three cells in each hemisphere for the terrestrial case $\Omega/\Omega_0 = 1$, and multiple cells for $\Omega/\Omega_0 = 3$. The scale of the cells is approximately inversely proportional to Ω. At the equator, zonal winds are easterly in the lower layers, while there exist weak westerlies in the upper troposphere (Figs. 2d–f). In the mid-latitudes, westerlies prevail from the top to the bottom layers. Because of the existence of non-axisymmetric modes, the angular momentum is effectively transported downward in comparison to 2D. The surface winds near the poles are easterly for $\Omega/\Omega_0 = 1$, where polar direct cells exist. As shown by Fig. 3, the time variability of the surface zonal winds for $\Omega/\Omega_0 = 1$ is smaller than that for 2D. In particular, in 3D, the position of the boundary of westerly and easterly, which corresponds to the subtropical high pressure, is located at almost a definite latitude (about 28°; Fig. 3b).

Fig. 4 shows the meridional angular momentum fluxes,

$$\begin{aligned} &2\pi a^2 \cos^2\varphi \int_0^{p_s} [\overline{uv}] \frac{dp}{g} \\ &= 2\pi a^2 \cos^2\varphi \int_0^{p_s} [\overline{u'v'}] \frac{dp}{g} \\ &+ 2\pi a^2 \cos^2\varphi \int_0^{p_s} [\bar{u}][\bar{v}] \frac{dp}{g}, \end{aligned} \tag{2}$$

for 2D and 3D, where p is the pressure, p_s the surface pressure, a the radius of the earth, g the acceleration of gravity, u the zonal wind and v the meridional wind. [ ] is the time average, $\overline{(\ )}$ is the zonal average, and $'$ is the departure from the zonal average. Total momentum transports for 3D are shown by solid lines, eddy components by dotted lines, transports due to zonal mean winds by dashed lines, and total transports for 2D by dashed and dotted lines; these are abbreviated as $[\overline{uv}]$, $[\overline{u'v'}]$, $[\bar{u}][\bar{v}]$, and $[uv]_{2D}$, respectively. Following points are noted:

- Total angular momentum transports for 3D are greater than those for 2D by a factor of 2–4. However, the latitudinal widths in which $[uv]_{2D}$ and $[\bar{u}][\bar{v}]$ have significant values are comparable.

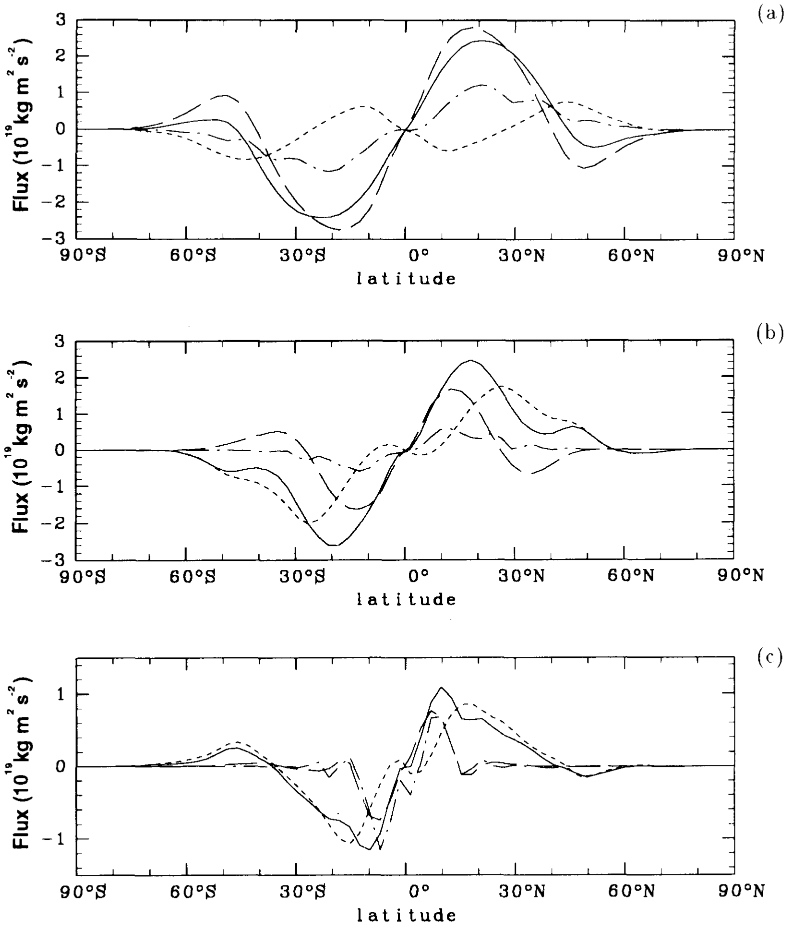

Fig. 4. Latitudinal distributions of angular momentum transports for (a) $\Omega/\Omega_0 = 1/3$, (b) $\Omega/\Omega_0 = 1$, and (c) $\Omega/\Omega_0 = 3$. Solid lines: total transports for 3D ($[\overline{uv}]$), dotted lines: eddy components ($[\overline{u'v'}]$), dashed lines: transports due to zonal mean winds ($[\bar{u}][\bar{v}]$), dashed and dotted lines: total transports for 2D ($[uv]_{2D}$). Unit is 10^{19} kg m^2 s^{-2}.

• The Hadley cell is interconnected with the Ferrel cell through $[\overline{u'v'}]$. The maximum value of $[\overline{u'v'}]$ is located near the boundary of both cells.

• The transport due to the eddy component $[\overline{u'v'}]$ is equatorward in the low-latitudes, and maintains the equatorial upper westerlies.

• The cells on the polar sides of the Ferrel cells have little interaction with the Hadley cell. In particular, in the case of $\Omega/\Omega_0 = 3$, both westerlies and easterlies exist at the surface layer of each successive cell in the mid- and high-latitudes, and inflows and outflows of angular momentum occur at the surface boundary of the cells.

As for the angular momentum budget in 3D, the angular momentum is supplied from the ground in the Hadley region of the surface easterlies and is transported upward by the Hadley cell in the same manner as in 2D. In 3D, however, the eddy components transport the angular momentum to the mid-latitudes and the Ferrel cell transports it downward. Eventually, it is transferred from the atmosphere to the earth in the region of the surface westerlies in the mid-latitudes. The contribution of the direct cells near the poles to the global budget is small in the terrestrial condition.

At the end of this section, a PV-θ view of the experiments is mentioned. Fig. 5 shows the meridional distributions of the potential vorticity PV and the potential temperature θ. Here,

$$\mathrm{PV} = -g\zeta_{a\theta}\frac{\partial\theta}{\partial p}, \tag{3}$$

where $\zeta_{a\theta}$ is the vertical component of the isentropic absolute vorticity, that is, the vorticity with horizontal derivatives evaluated on isentropic surfaces (Hoskins et al., 1985; Hoskins, 1991). In 2D, it is expressed by

$$\begin{aligned}\zeta_{a\theta} &= 2\Omega \sin\varphi + \frac{1}{a\cos\varphi}\left(\frac{\partial u\cos\varphi}{\partial\varphi}\right)_\theta \\ &= \frac{1}{a^2\cos\varphi}\left(\frac{\partial l}{\partial\varphi}\right)_\theta,\end{aligned} \tag{4}$$

where $l = ua\cos\varphi + \Omega a^2\cos^2\varphi$ is the angular momentum.

The contour intervals of PV in Fig. 5 are $\Omega_0/\Omega \times 10^{-7}\ \mathrm{m^2\,K\,s^{-1}\,kg^{-1}}$ ($0.1 \times$ PV-unit normalized by the terrestrial rotation rate). In 2D (a)–(c), θ is horizontally uniform in the Hadley region, and is vertically uniform in the troposphere of the mid- and high-latitudes. PV is almost zero in both regions, since the angular momentum is conserved in the Hadley region, and stratification is neutral in the troposphere of the mid- and high-latitudes. Between both regions around the polar boundary of the Hadley cell, PV has a large gradient and the contours of PV are almost parallel to the contours of θ. The distribution of θ clearly shows the tropopause level, which exists near the contour of PV $= 1.0$ PVU $\times\ \Omega_0/\Omega$. The tropopause level in the low-latitudes is determined by the moist radiative-convective equilibrium in the whole region of the Hadley cell, and the level in the mid- and high-latitudes is determined by the local radiative-convective equilibrium in each latitude (Satoh, 1994).

Figs. 5d–f show PV-θ for 3D. Although the distributions of PV and θ in the Hadley cell are similar to 2D, the gradient of PV near the cell boundary is reduced. In the mid- and high-

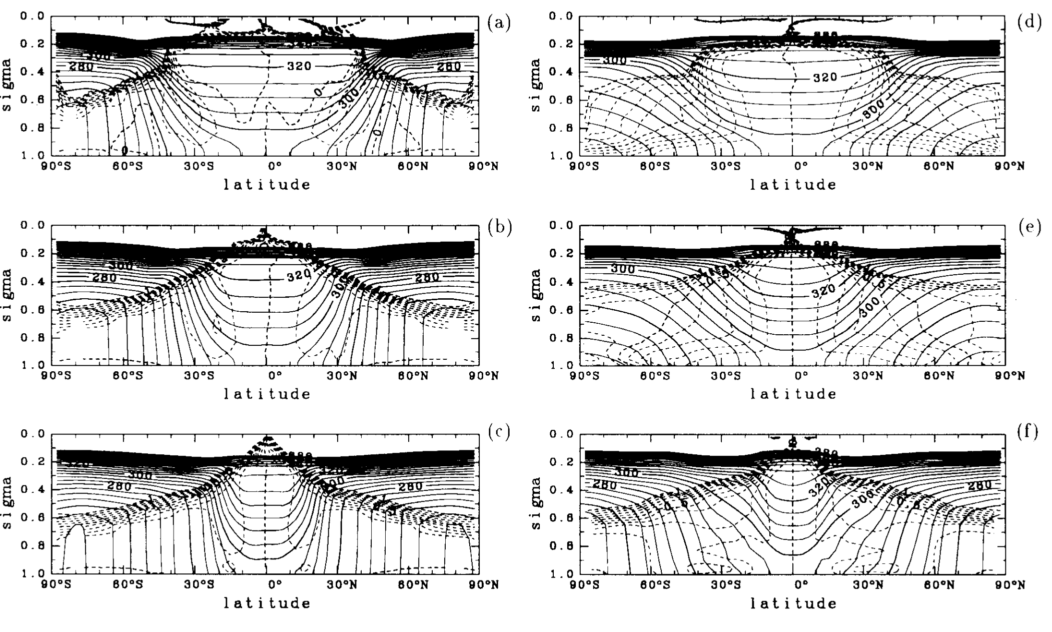

Fig. 5. Meridional distributions of potential temperature and potential vorticity for (a) 2D, $\Omega/\Omega_0 = 1/3$, (b) 2D, $\Omega/\Omega_0 = 1$, (c) 2D, $\Omega/\Omega_0 = 3$, (d) 3D, $\Omega/\Omega_0 = 1/3$, (e) 3D, $\Omega/\Omega_0 = 1$, and (f) 3D, $\Omega/\Omega_0 = 3$. Solid lines are the potential temperature and dashed lines are the potential vorticity. Contours for the potential temperature range up to 380 K with intervals of 5 K. Contours for the potential vorticity range from -1.0 to $+1.0$ PVU $\times\ \Omega_0/\Omega$ with intervals of 0.1 PVU $\times\ \Omega_0/\Omega$ (PVU $= 10^{-6}\ \mathrm{m^2\,K\,s^{-1}\,kg^{-1}}$).

latitudes, the contours of θ decline and cross the ground, and PV has a non-zero value as a result of the stable stratification. Fig. 5e shows that the contours of PV (with intervals of 0.1 PVU) are crossing with the contour 300 K at 0°, 11°, 18°, 27°, 37°, and 42°. This indicates that the gradient of PV is almost zero in the upward motion region of the Hadley cell, relatively large in the downward motion region, relatively small in the extratopic troposphere, and very large in the extratopic stratosphere. These are consistent with Fig. 1 of Sun and Lindzen (1994). In the extratopic troposphere, however, these figures do not support their view in which PV is homogenized along isentropic surfaces by baroclinic adjustment. As shown by the contour of PV $= 1.0$ PVU $\times \Omega_0/\Omega$, the tropopause level does not change in the Hadley region, while it becomes higher by 100 hPa than that for 2D in the mid- and high-latitudes except for the case $\Omega_0/\Omega = 3$. The tropopause level for 3D may be affected by baroclinic instability as stated by Lindzen (1993). Although the dependency on the rotation rate is not well understood, the tropopause level at the pole seems to change in accordance with the meridional scales of polar cells.

4. Discussion

In this section, relations of the Hadley to Ferrel cells are discussed. Fig. 6 shows the dependencies

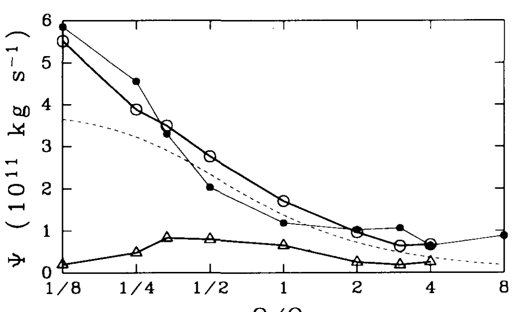

Fig. 6. Dependencies of the intensities of the Hadley and Ferrel cells on the rotation rates. Thick line with open circles: the Hadley cell for 3D, Ψ_H, thick line with open triangles: the Ferrel cell for 3D, Ψ_F, thin line with closed circles: the Hadley cell for 2D, Ψ_H, and dotted line: the Hadley cell by the simple model, Ψ_H. Unit in the vertical scale is 10^{11} kg s^{-1}.

of the cell intensities on the rotation rates, where the intensities are defined by the maximum values of the stream functions. The Hadley cells in 3D are slightly stronger than those in 2D in the cases around $\Omega/\Omega_0 = 1$. This is because the Hadley cell in 2D is unsteady, since the moving symmetric cells invade the Hadley region (Fig. 3b). To a first approximation, however, they take almost the same values, and it is suggested that the intensity of the Hadley cell in 3D can be given by the simple axisymmetric model by Held and Hou (1980) or by the moist radiative-convective version by Satoh (1994).

The intensity of the Hadley cell Ψ_H is expressed by

$$\Psi_H = 2\pi a^2 M^d \sin \varphi_H, \tag{5}$$

which can be obtained by multiplying eq. (31) of Satoh by $2\pi a$, and by setting $\mu = 0$. M^d is the downward mass flux in the Hadley cell, and φ_H is the width of the cell, given by

$$M^d = \frac{Q^{rad} H}{L q_B(0)}, \tag{6}$$

$$\sin \varphi_H = \left(\frac{2R}{1+2R}\right)^{1/2}, \tag{7}$$

$$R = \frac{gH}{\Omega^2 a^2} \frac{\Delta T}{T_0}, \tag{8}$$

which corresponds to eq. (30), (45), and (46) of Satoh, respectively. Here, eq. (7) is the limit $r_1 \ll 1$ of eq. (46) of Satoh. Q^{rad} is the radiative cooling rate, $q_B(0)$ the specific humidity in the boundary layer at the equator, ΔT the difference of the surface temperature from equator to pole, T_0 the mean temperature, H the tropopause height, and L the latent heat (Lindzen et al., 1982; Satoh and Hayashi, 1992). In these experiments, eq. (6) is not useful in determining the value of M^d, since Q^{rad} is not an external parameter. From the stream functions (Fig. 1), the values of M^d are estimated to be 0.0010–0.0025 kg s^{-1} m^{-2}; M^d is smaller as Ω becomes larger. The dotted line of Fig. 6 is Ψ_H calculated by using eq. (5) with $M^d = 0.0015$ kg s^{-1} m^{-2}. This implies that the simple model reproduces the dependencies of the intensities of the Hadley cell for 2D and 3D on the rotation rates. It should be remembered here that the Hadley width for 2D is not uniquely defined, since it is broader at higher levels. In eq. (7) of the simple model, φ_H must be regarded as the cell width of the most upper troposphere, i.e., the largest width of the cell (Satoh, 1994). It is most clearly defined by the distribution of the potential temperature in Fig. 4.

Fig. 6 also implies that the intensity of the Ferrel cell is about half of the intensity of the Hadley cell in the cases of $\Omega/\Omega_0 > 1/3$. The relation of the intensities of the two cells is given as follows by using the angular momentum budget. The upward transport of the angular momentum in the Hadley cell is balanced by the downward transport in the Ferrel cell. The horizontally averaged budget at the middle of the troposphere is written as

$$\Psi_H \, \Delta l_H + \Psi_F \, \Delta l_F = 0, \tag{9}$$

where Ψ_H and Ψ_F are the maximum values of the mass stream functions of the Hadley and Ferrel cells, respectively, and Δl_H and Δl_F are the differences of the angular momentums between the upward and downward branches in the respective cells. In this equation, the Lagrangian transport of the angular momentum is considered in the Hadley part, whereas only the contribution due to the mean meridional flow is taken into account in the Ferrel part by following Phillips (1954). If the angular momentums in eq. (9) is estimated by the value near the surface boundary, it is given by the rigid body components ($u = 0$) as

$$l = \Omega a^2 \cos^2 \varphi. \tag{10}$$

If $\Delta\varphi_H$, $\Delta\varphi_F \ll 1$ is assumed for simplicity, where $\Delta\varphi_H (= \varphi_H)$ and $\Delta\varphi_F$ denote the latitudinal widths of the Hadley and Ferrel cells, respectively, the difference in the Hadley region, $0 < \varphi < \Delta\varphi_H$, is

$$\begin{aligned} \Delta l_H &= -\Omega a^2 \sin^2(\Delta\varphi_H) \\ &\approx -\Omega a^2 \, \Delta\varphi_H^2, \end{aligned} \tag{11}$$

whereas the difference in the mid-latitude, $\Delta\varphi_H < \varphi < \Delta\varphi_H + \Delta\varphi_F$, is, by using $\Delta \cos^2 \varphi \approx -2 \sin \varphi \cos \varphi \, \Delta\varphi$,

$$\begin{aligned} \Delta l_F &\approx -2\Omega a^2 \sin(\Delta\varphi_H) \cos(\Delta\varphi_H) \, \Delta\varphi_F \\ &\approx -f a^2 \, \Delta\varphi_F, \end{aligned} \tag{12}$$

where $f = 2\Omega \sin(\Delta\varphi_H) \approx 2\Omega \, \Delta\varphi_H$ is the Coriolis factor. Letting $\Delta y = a \, \Delta\varphi_F$ denote the north-south length of the Ferrel cell, one obtains $\Delta l_F = -f \, \Delta y a$, which corresponds to the difference of the angular momentum in the f-plain, $u - fy$, multiplied by a. From this, one can confirm the second term of eq. (9) is derived from the Coriolis term of the equation of the zonal wind. Substitution of eqs. (11)–(12) to eq. (9) yields

$$\frac{\Psi_F}{\Psi_H} = -\frac{\Delta\varphi_H}{2 \, \Delta\varphi_F}. \tag{13}$$

In 3D, in contrast to 2D, the cell widths, $\Delta\varphi_H$ and $\Delta\varphi_F$, are uniquely defined, since they do not depend on heights. Because the regions of the surface easterlies and westerlies correspond to the Hadley and Ferrel cells, respectively, the boundaries of the cells may be most clearly defined by the latitudes at which the surface winds vanish ($[\bar{u}] = 0$ at $z = 0$).

The Hadley cell in 2D spreads over the polar side region of the latitude of $[\bar{u}] = 0$ at $z = 0$ (the sub-tropical high) and the upper level poleward flows maintain strong westerlies and strong baroclinicity. It may regarded that the baroclinic waves in 3D develop in these latitudes, and that the region of the Ferrel cell corresponds to this strong baroclinic zone. One therefore has $\Delta\varphi_H \approx \Delta\varphi_F$ and $-\Psi_F/\Psi_H \approx 1/2$, to a first approximation.

Fig. 7 compares the ratios $-\Psi_F/\Psi_H$ and $\Delta\varphi_H/2 \, \Delta\varphi_F$. Only in the cases of $\Omega/\Omega_0 \approx 1$, the dependencies on Ω are similar. For $\Omega/\Omega_0 < 1/3$, the approximation $\varphi_H \ll 1$ breaks down. For $\Omega/\Omega_0 > 3$, the Ferrel cell is affected by the cells in the higher latitudes; the angular momentum budget does not close within the Hadley–Ferrel system (Fig. 4c), and the inflow from the ground in

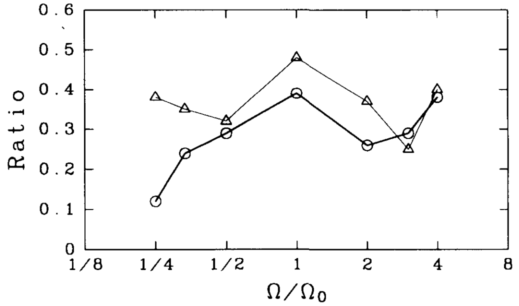

Fig. 7. Dependencies of the ratios of the intensities of the Ferrel cell to those of the Hadley cell ($-\Psi_F/\Psi_H$: circles) and of the cell widths ($\Delta\varphi_H/2 \, \Delta\varphi_F$: triangles) on the rotation rates.

the regions of the surface easterlies in the mid- and high-latitudes becomes non-negligible.

To this point, experiments have been performed on the same surface temperature distribution given by eq. (1). One may ask how the arguments would change if the surface temperatures were differently distributed. In order to particularly explore the influence of the equatorial surface temperature distributions on the Hadley cell, further calculations have been done under the condition,

$$T_s = T_e - \Delta T \sin^n \varphi, \tag{14}$$

with the index n varied from 2 to 3 and 4. (The case $n = 2$ is the same as eq. (1).)

Fig. 8 shows the meridional distributions of the mass stream functions at the level $\sigma = 0.7$ for $n = 2$, 3, and 4. (The results for $n = 2$ correspond to Figs. 1c and g.) At first sight of Fig. 8a, the intensities and the widths of the Hadley cell for 2D do not change. However, the cell shapes for $n = 3$ and 4 are more like rectangulars, and the cell width is almost constant irrespective of height (figures are not shown). The stream functions for $n = 3$ and 4 attain their maximum values at $\sigma \approx 0.7$, while it is at the higher level $\sigma \approx 0.5$ for $n = 2$ (Fig. 1c). The simple axisymmetric theory expects that no clear Hadley cells will exist in the case of $n \geqslant 4$ (Plumb and Hou, 1992). In this study, however, the Hadley cell exists even for $n = 4$, so that a different explanation for the Hadley cell is required. Since the surface temperatures near the equator are rather uniform if n is large, the Hadley cell should be viewed as a large scale moist circulation system on a uniform surface temperature. Their behaviors are very sensitive to model parameters, and the cause of the circulation systems under such a condition is not well understood.

Fig. 8b shows the results for $n = 2$, 3 and 4 for 3D. The intensities of the Hadley cell for $n = 3$ and 4 are smaller than that for $n = 2$ and are comparable to that for 2D. However, the cell widths are broader than the widths for 2D: 30° versus 15°. This suggests that the Hadley cells are controlled by different dynamics between 2D and 3D for large n. The dynamics is speculated as follows, though this view is tentative and requires additional experiments to confirm. There is a baroclinicity in the mid-latitudes corresponding to the surface temperature gradient even for $n = 3$ and 4.

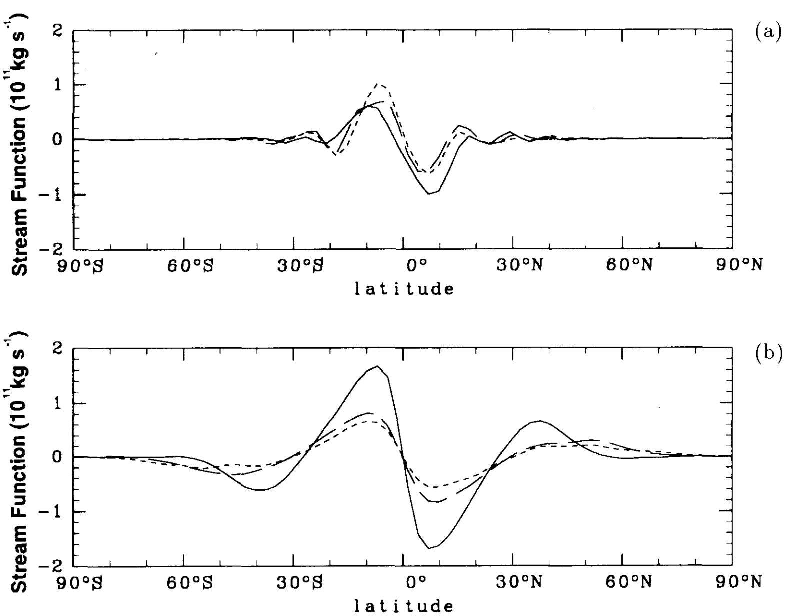

Fig. 8. Latitudinal distributions of the mass stream functions at $\sigma = 0.70$ for (a) 2D and (b) 3D, $\Omega/\Omega_0 = 1$; solid lines: $n = 2$, dashed lines: $n = 3$, and dotted lines: $n = 4$, where n is the index in the surface temperature distribution eq. (14). Unit is 10^{11} kg/s.

In 3D, the Ferrel cell, which is a result of baroclinic instability in the mid-latitudes, transports the angular momentum downwards. In order to balance the downward transport, the upward transport is induced in the other latitudes, and, as a result, a direct cell will be driven especially in the lower latitudes because of the geometry of the sphere. In this manner, the Hadley cells for $n=3$ and 4 of 3D may be viewed as another type of the circulations, which are induced by the baroclinic waves as in the classical theory of Phillips (1954). In summary of this speculation, as the equatorial surface temperature gradient is smaller, the Hadley cell tends to be affected by the activity of the baroclinic waves in the mid-latitudes, and the simple axisymmetric theory becomes less applicable. In any case, the interaction of the angular momentum transport between the Hadley and Ferrel cells remains important.

5. Summary and further comments

In this study, general circulations in the two-dimensional axisymmetric and the three-dimensional asymmetric experiments are compared under the same axisymmetric boundary conditions. Under the standard surface temperature distribution eq. (1), the Hadley cell behaves similarly; the intensities and the cell widths are comparable between 2D and 3D. The basic properties of the Hadley cell in 3D can be described by the simple axisymmetric theory (Held and Hou, 1980; Satoh, 1994). The most distinct difference is in its shape; in 2D, the cell width is broader at higher altitudes, while, in 3D, it does not depend on height.

Circulations in the mid-latitudes are essentially different. In 2D, a symmetric multiple cellar structure exists. The cells are systematically moving equatorward, and they transport the angular momentum downward. The time averaged surface zonal winds almost vanish and a strong westerly shear appears in the mid-latitudes. In 3D, on the other hand, since baroclinic waves exist, zonal mean winds are westerly from the surface to the upper troposphere in the mid-latitudes and the westerly shear is relatively weaker. This suggests that baroclinic waves in 3D efficiently transport angular momentum downward in comparison to the symmetric cells in 2D.

One must note, however, that the behaviors of the Hadley cell is not always explainable in the framework of 2D. Contrary to the expectation obtained from the simple axisymmetric theory that the Hadley cell no longer exists if the gradient of the surface temperature near the equator is sufficiently weak (Plumb and Hou, 1992), numerical results show that there exists a weak but clear cell both in 2D and 3D. Although their intensities are almost the same, the cell width is broader in 3D than in 2D, and this suggests that the cells are controlled by different dynamics. Instead of the simple axisymmetric theory, the theory of the meridional circulations of the quasi-geostrophic model by Phillips (1954) is more applicable to this case of 3D; the Hadley cell is induced by the baroclinic waves in the mid-latitudes.

The Hadley cell is characterized by two extreme views; one described by the simple axisymmetric theory (referred to as the SH-type), and the other not described in the axisymmetric framework but induced by baroclinic waves (referred to as the QH-type). The type of the Hadley cell depends on the latitudinal gradient of the surface temperature in the low-latitudes. The Hadley cell in the real atmosphere is thought to have both characters, since the gradient is fairly moderate especially in the western Pacific. In the extreme former type (SH), the Hadley cell is induced by the strong gradient of the equatorial surface temperature. Since the surface winds are easterly in the Hadley region, the angular momentum is pumped up from the ground to the atmosphere, and transported to the mid-latitudes. This transport maintains baroclinicity in the mid latitudes, and, in order to balance it, a downward transport of the angular momentum due to baroclinic instability is induced. Therefore, the activity of the baroclinic waves in the mid-latitudes is thought to be passively determined by the Hadley cell. In the other extreme (QH), on the contrary, the Hadley cell is passively determined by the baroclinic waves. At first, the surface temperature gradient in the mid-latitudes maintains baroclinicity in this region. Baroclinic instability reduces the baroclinicity and transports the angular momentum downward. There must be a supply of angular momentum from the other latitudes to balance it. The transport from the lower latitudes plays a major role in comparison to one from the higher latitudes owing to the geometric effect of the sphere. Thus, the direct cell in the low-latitudes (the Hadley cell) is reinforced and transports the angular momentum upward.

In either type, the Hadley cell is related with the Ferrel cell in terms of the angular momentum budget. It has been shown that the ratio of the intensity of the Ferrel cell to that of the Hadley cell is given by their latitudinal widths (eq. (13)). The ratio is about half if the cell widths are assumed to be equal. In the SH-type, in particular, it may be possible to estimate, by using theories of baroclinic instability, amplitudes of the baroclinic waves and latitudinal energy transports by them in terms of external parameters, since the intensity of the Hadley cell is given by the simple axisymmetric theory. Although it is true that these estimations are very crude and limited, one should be reminded that the angular momentum requirement is useful in discussing the interactions between the Hadley cell and the baroclinic waves.

Here, some unresolved problems concerning the above discussions will be commented upon. First, development of theories on the cell widths relationship is required. According to the numerical results, the region of the Ferrel cell in 3D corresponds to those of the strong baroclinicity in 2D (the upper and the polar part of the Hadley cell). It is not, however, a logical consequence that the position of the Ferrel cell in 3D agrees with that of the baroclinicity in 2D. The transport of the angular momentum between the Hadley and Ferrel cells in 3D is due to the eddy components, such as Rossby waves, and will be associated with the life cycle of extratropical cyclones. Numerical experiments by Simmons and Hoskins (1978, 1980) show that the latitudinal transport of the angular momentum is caused by the propagation of Rossby waves from the mid-latitude baroclinic zones and the successive absorption or breaking in the low-latitudes (Held and Hoskins, 1985). In their experiments, however, westerly shears are assumed to be placed in the mid-latitudes as initial conditions. In order to determine the position of the westerly shear, i.e., the baroclinic zone, balance among the tranports of the Hadley cell, the Rossby waves, and the baroclinic waves should be considered. In the case of the SH-type, the Hadley cell will play a dominant role in this balance, since the outflow of the angular momentum from the Hadley region is required as in the framework of 2D.

Second, in the QH-type circulation, how do the baroclinic waves affect the cumulus activity in the tropics? In this case, the baroclinic instability is prescribed in the mid-latitudes, and the Rossby waves are thought to be generated from this region. Absorption of the Rossby waves decelerates the zonal winds in the low-latitudes, and results in a meridional circulation and redistribution of mass through geostrophic adjustment. This can also be viewed by the downward control principle (Haynes et al., 1991). The large scale circulation thus induced will have an influence on the tropical cumulus activity in some ways. It will be difficult, however, to extract this kind of mechanism from the observational data.

Dependencies on the rotation rates further suggest possible classification of the baroclinic zones. If the rotation rate is large, more than three cells exist in the mid- and high-latitudes. Since the polar cells have little interaction with the Hadley cell, the internal dynamics of the baroclinic waves determine the intensities and the widths of the cells. Thus, the baroclinic zones may be classified into two groups: one where interaction of the angular momentum transport with the Hadley cell is significant, and the other where the interaction is insignificant. The former type corresponds to the Ferrel cell by definition, and its property can be discussed in terms with the Hadley cell as described so far. The subtropical baroclinic zone of the earth has this character. On the other hand, the polar baroclinic zone has the latter character; it does not have a direct interaction with the Hadley cell. In order to systematically investigate the baroclinic zones of this type, much more complicated discussions will be required on the scales of cell widths, the number of cells, or the number of jets in the systems of high rotation rates. The baroclinic instability in the basic zonal winds of the multiple jets and its latitudinal transport of the angular momentum, and resulting zonal wind redistribution should be at once considered. In the present stage, a full analysis of the baroclinic waves calculated with a high rotation rate is required, since such an analysis has not been performed up to now. Experiments of this kind would certainly provide a useful information for discussing properties of the baroclinic zones of the earth.

6. Acknowledgments

This work was supported by the Japan Society for the Promotion of Science and the Center for the Climate System Research, University of Tokyo. Numerical calculations were performed with HITAC S-3800 and M-880 at the Computer Center of the University of Tokyo, and NEC SX-3 at the National Institute for Environmental Studies. Figures were produced by GFD-DENNOU libraries and GTOOL3 by Dr. Numaguti.

REFERENCES

Eliassen, A. 1951. Slow thermally or frictionally controlled meridional circulation in a circular vortex. *Astrophys. Norv.* **5**, 19–60.

Emanuel, K. A. 1979. Inertial instability and mesoscale convective systems. Part I: Linear theory of inertial instablity in rotating viscous fluids. *J. Atoms. Sci.* **36**, 2425–2449.

Emanuel, K. A. 1982. Inertial instability and mesoscale convective systems. Part II: Symmetric CISK in a baroclinic flow. *J. Atmos. Sci.* **39**, 1080–1097.

Haynes, P. H., McIntyre, M. E., Shepherd, T. G. and Shine, K. P. 1991. On the "downward control" of extratropical diabatic circulations by eddy-induced mean zonal forces. *J. Atmos. Sci.* **48**, 651–678.

Held, I. M. and Hoskins, B. J. 1985. Large-scale eddies and the general circulation of the troposphere. *Advances in Geophys.* **28**, 3–31.

Held, I. M. and Hou, A. Y. 1980. Nonlinear axially symmetric circulations in a nearly inviscid atmosphere. *J. Atmos. Sci.* **37**, 515–533.

Hoskins, B. J. 1991. Towards a PV-theta view of the general circulation. *Tellus* **43A/B**, 27–35.

Hoskins, B. J., McIntyre, M. E. and Robertson, A. W. 1985. On the use and significance of isentropic potential vorticity maps. *Q. J. R. Meteorol. Soc.* **111**, 877–946.

Lindzen, R. S. 1993. Baroclinic neutrality and the tropopause. *J. Atmos. Sci.* **50**, 1148–1151.

Lindzen, R. S., Hou, A. Y. and Farrell, B. F. 1982. The role of convective model in calculating the climate impact of doubling CO_2. *J. Atmos. Sci.* **39**, 1189–1205.

Numaguti, A. 1993. Dynamics and energy balance of the Hadley circulation and the tropical precipitation zones: significance of the distribution of evaporation. *J. Atmos. Sci.* **50**, 1874–1887.

Palmén, E. and Newton, W. 1969. *Atmospheric circulation systems*. Academic Press, 603 pp.

Phillips, N. A. 1954. Energy transformations and meridional circulations associated with simple baroclinic waves in a two-level, quasi-geostrophic model. *Tellus* **4**, 3273–286.

Plumb, A. and Hou, A. Y. 1992. The response of a zonally-symmetric atmosphere to subtropical thermal forcing: threshold behavior. *J. Atmos. Sci.* **49**, 1790–1799.

Satoh, M. 1994. Hadley circulations in radiative-convective equilibrium in an axially symmetric atmosphere. *J. Atmos. Sci.* **51**, 1947–1968.

Satoh, M. and Hayashi, Y.-Y. 1992. Simple cumulus models in one-dimensional radiative convective equilibrium problems. *J. Atmos. Sci.* **49**, 1202–1220.

Schneider, E. K. 1977. Axially symmetric steady-state models of the basic state for instability and climate studies (II). Nonlinear calculations. *J. Atmos. Sci.* **34**, 280–296.

Simmons, A. J. and Hoskins, B. J. 1978. The life cycles of some nonlinear baroclinic waves. *J. Atmos. Sci.* **35**, 414–432.

Simmons, A. J. and Hoskins, B. J. 1980. Barotropic influences on the growth and decay of nonlinear baroclinic waves. *J. Atmos. Sci.* **37**, 1679–1684.

Stone, P. H. 1966. On non-geostrophic baroclinic stability. *J. Atoms. Sci.* **23**, 390–400.

Sun, D.-Z. and Lindzen, R. S. 1994. A PV view of the zonal mean distribution of temperature and wind in the extra-tropical troposphere. *J. Atmos. Sci.* **51**, 751–772.

Williams, G. P. 1988a. The dynamics range of global circulations (I). *Climate Dynamics* **2**, 205–260.

Williams, G. P. 1988b. The dynamics range of global circulations (II). *Climate Dynamics* **3**, 45–84.